

A Comparative Study of Scanpath Models in Graph-Based Visualization

Angela Lopez-Cardona
angela.lopez.cardona@telefonica.com
Telefónica Scientific Research
Barcelona, España
Universitat Politècnica de Catalunya
Barcelona, España

Parvin Emami
parvin.emami@uni.lu
University of Luxembourg
Esch-sur-Alzette, Luxembourg

Sebastian Idesis
sebastianariel.idesis@telefonica.com
Telefónica Scientific Research
Barcelona, España

Saravanakumar Duraisamy
saravanakumar.duraisamy@uni.lu
University of Luxembourg
Esch-sur-Alzette, Luxembourg

Luis A. Leiva
luis.leiva@uni.lu
University of Luxembourg
Esch-sur-Alzette, Luxembourg

Ioannis Arapakis
ioannis.arapakis@telefonica.com
Telefónica Scientific Research
Barcelona, España

Abstract

Information Visualization (InfoVis) systems utilize visual representations to enhance data interpretation. Understanding how visual attention is allocated is essential for optimizing interface design. However, collecting Eye-tracking (ET) data presents challenges related to cost, privacy, and scalability. Computational models provide alternatives for predicting gaze patterns, thereby advancing InfoVis research. In our study, we conducted an ET experiment with 40 participants who analyzed graphs while responding to questions of varying complexity within the context of digital forensics. We compared human scanpaths with synthetic ones generated by models such as DeepGaze, UMSS, and Gazeformer. Our research evaluates the accuracy of these models and examines how question complexity and number of nodes influence performance. This work contributes to the development of predictive modeling in visual analytics, offering insights that can enhance the design and effectiveness of InfoVis systems.

This is the author's version of this work, provided for personal use only. Redistribution is prohibited. The definitive, published version is available in the ACM ETRA Conference Proceedings, ISBN 979-8-4007-1487-0/2025/05, <https://doi.org/0.1145/3715669.3725882>.

1 Introduction

Information visualization (InfoVis) systems rely on visual elements like charts, graphs, networks, and maps to derive intuitive insights from large datasets, by engaging our visual system's capacity for sensing differences rather than making laborious comparisons between data elements [Wang et al. 2024b]. In today's information-saturated environment, users must decide what to process, filter, and prioritize. Although using visualizations to address this challenge has been widely discussed [Perkhofer et al. 2016], InfoVis systems have yet to fully realize their potential in aiding critical decision-making. The effectiveness of InfoVis in responding to critical events hinges on the visual representation of data and the speed at which actionable insights can be derived. We argue that physiological computing holds significant promise for innovation in InfoVis by incorporating human body signals, which can lead to

more precise user interface adaptations through closed-loop implicit monitoring [Fairclough 2022]. This is supported by evidence that cognitive processes are affected by user interface aesthetics, detectable through physiological signals [Haddad et al. 2024; Hirshfield et al. 2011; Lukanov et al. 2016; Peck et al. 2013]. Specifically, visual attention allocation in graphic design reflects the perceived importance of design elements [Cartella et al. 2024]. Understanding how users allocate their attention presents a research opportunity [Emami et al. 2024].

In the context of visual attention, we can differentiate between bottom-up saliency, which arises from low-level visual features like color, contrast, and motion, capturing attention automatically. In contrast, top-down saliency is shaped by prior knowledge, tasks, and goals, guiding attention based on relevance [Wang et al. 2024a]. While bottom-up saliency is driven by stimuli, top-down saliency is cognitive and context-dependent [Wang et al. 2024a]. InfoVis mainly involves top-down processing as users engage with visual representations [Wang et al. 2024a].

To model visual attention, Eye-tracking (ET) is typically used. However, collecting organic data presents significant challenges, including the reliance on proprietary, high-precision equipment and data privacy concerns [Khurana et al. 2023]. Recent studies have addressed the limitations of ET technology by introducing computational attention models, a promising alternative to predict gaze patterns in response to specific stimuli [Deng et al. 2023]. In the field of Computer Vision (CV), predictive models of human attention have demonstrated their utility across various applications, including the optimization of interaction designs and the enhancement of webpage layouts [Li et al. 2024]. To train and evaluate these models, scientific datasets containing fixation points generated by human observers exploring images on specific tasks have been developed. These datasets are typically captured using eye-trackers, webcams [Assens et al. 2018] and mouse clicks with techniques like BubbleView [Kim et al. 2017]. Popular examples are MASSVIS [Borkin et al. 2016], and UEye dataset [Jiang et al. 2023a] for InfoVis and SALICON [Jiang et al. 2015] and CAT2000 [Borji and Itti 2015] for natural images.

Typically, existing solutions predict either visual attention [Aydemir et al. 2023; Chen et al. 2023; Fosco et al. 2020a], also referred to as saliency modeling, or scanpaths, which is also regarded as

another form of saliency prediction that accounts for the temporal dimension [Kümmerer et al. 2022; Martin et al. 2022; Sui et al. 2023; Wang et al. 2024a]. Saliency prediction aims to generate heatmaps or probability distributions that emphasize areas of attention within an image [Cartella et al. 2024]. Contemporary approaches utilize deep neural networks to automatically learn discriminative features, as evidenced by models such as those proposed by Chen et al. [2023] and Aydemir et al. [2023]. Aydemir et al. [2023].

However, collapsing attention prediction to saliency maps results in the loss of temporal information of attentional deployment [Cartella et al. 2024]. Two scanpaths that cover similar areas of an image, but follow entirely different sequences, can yield identical saliency maps. Nevertheless, the order in which a visual stimulus is explored is important, as it more accurately reflects the prominence of the image elements in relation to the observer [Cartella et al. 2024]. This has driven research into the complementary task of scanpath prediction—the task of forecasting a sequence of fixations over a visual stimulus. Certain models for predicting scanpaths in images have been proposed, with recent efforts placing more emphasis on deep learning solutions (e.g., TPP-Gaze [D’Amelio et al. 2024]). While most models are based on free-viewing human scanpaths, the former ones emerge for InfoVis [Wang et al. 2024a]. Specific models are needed since InfoVis stimuli are fundamentally different from natural images: they typically include more text and larger areas with uniform color and minimal to no texture [Matzen et al. 2018; Wang et al. 2024a].

By modeling eye movement patterns based on visual saliency, we can gain insights into user perception and interaction, reducing the need to involve users early in the design process [Emami et al. 2024; Shi et al. 2025]. These predictions enable us to measure the impact of visual changes in InfoVis, optimize design components for specific attention levels, and evaluate user awareness of elements over time [Emami et al. 2024]. Such solutions could be used as an evaluation tool, which visualization designers can use to compare candidate designs in either a qualitative or quantitative manner [Matzen et al. 2018]. Modelling scanpaths on InfoVis can offer insights into the rich spatial and temporal dynamics of human attention [Wang et al. 2024a].

In this paper, we conducted a ET study with 40 participants who analysed graphs of different numbers of nodes, while answering questions of varying complexity in the context of digital forensics. We investigated how similar these gaze patterns are to synthetic scanpaths produced by various generative models: DeepGaze [Kümmerer et al. 2022], UMSS [Wang et al. 2024a] and Gazeformer [Mondal et al. 2023]. Our objective is to determine which state-of-the-art generative model can most effectively synthesise realistic scanpaths on graph-based visualizations and how the question and visualisation complexity impacts their accuracy.

2 Related work

Eye-tracking is extensively used in InfoVis as it offers valuable insights into information foraging and decision-making processes, thereby informing research on visual attention [Borkin et al. 2016] [Nguyen et al. 2017].

Considering the different conditions in visual analysis tasks, Polatsek et al. [2018] explored how visual attention and perception

influence task-based analysis. By examining the MASSVIS dataset, their study demonstrated that free-viewing saliency models fall short in capturing the nuances of task-driven attention, suggesting that these models require further refinement. Following that, Wang et al. [2024b] created the SalChartQA dataset, a human-annotated Chart Question Answering dataset covering three visualization types: bar plots, line plots, and pie charts. Analyses on SalChartQA demonstrate the strong impact of the question on visual saliency. However, this study does not analyze graph-based visualizations and collects data using BubbleView [Kim et al. 2017].

Early research on scanpath prediction has primarily utilized bottom-up saliency maps to predict gaze shifts and positions. Notable models, such as SalTiNet [Assens et al. 2017], introduced a deep learning framework that innovatively represents saliency maps in three dimensions, termed saliency volumes. This structure captures the temporal aspect of fixations by adding a temporal axis to traditional saliency maps. Scanpaths are generated by sampling fixation points from these saliency volumes, followed by a post-filtering stage. PathGAN [Assens et al. 2018] advanced this by offering a fully end-to-end solution, employing a generative adversarial network (GAN) to directly produce scanpaths without the need for sampling or post-processing. DeepGaze III [Kümmerer et al. 2022] improved prediction using saliency maps and previous scanpaths to forecast subsequent fixations, establishing itself as the state-of-the-art for generating free-viewing human scanpaths. Later, Jiang et al. [2023b] introduced DeepGaze++ based on DeepGaze III with modifications and fine-tuned it on the UEyes dataset. Emami et al. [2024] optimized the parameters of DeepGaze++, such as masking radius, IOR mechanisms and input image size for user interfaces, relevant to InfoVis. So we consider this version of DeepGaze++ as the state-of-the-art model for scanpath prediction with these parameters.

Recently, there has been a growing interest in visual attention models for InfoVis, as demonstrated by Matzen et al. [2018] who examined the limitations of existing saliency models on the MASSVIS dataset. Their findings motivated the development of the Data Visualization Saliency (DVS) model to better address these shortcomings. However, scanpath prediction remains underexplored, with UMSS [Wang et al. 2024a] emerging as the first notable contribution and serving as the state-of-the-art model in this area. Moreover, current methods typically generate visual attention maps without considering user questions or queries [Shi et al. 2025]. The investigation of goal-directed attention—such as that required for visual search tasks—remains in its early stages [Cartella et al. 2024]. In InfoVis, research on question-driven saliency and scanpath prediction is especially recent.

For saliency, VisSalFormer [Wang et al. 2024b] remains the only method available for predicting question-driven saliency on information visualizations. In terms of scanpaths, Chartist [Shi et al. 2025] is the only available model; it simulates how users move their eyes to forage information on a chart—handling tasks such as value retrieval, filtering, and identifying extremes. Although Chartist was developed around the same time as this work, its code was not available, so a direct comparison was omitted from our study. Moreover, since it is trained in a controlled environment rather than using human eye-tracking data, it opens a promising direction for future research.

Although these models are useful, they often depend on task-specific configurations that limit their generalizability. UniAR [Li et al. 2024] overcomes this by predicting scanpaths and saliency while also incorporating user input preferences across tasks. While promising, its closed-source nature prevented us from including it in our work.

3 Methodology

This section describes the methodology employed in this study, detailing the data collection process, the generative models used, and the evaluation metrics. The Data Collection subsection outlines participant recruitment Section 3.1.1, the stimuli used Section 3.1.2, task procedure Section 3.1.3, and the experimental apparatus Section 3.1.4. The Generative Models subsection introduces the models applied in the study Section 3.2 followed by a description of the metrics used for evaluation Section 3.3.

3.1 Data Collection

The data was collected with the purpose of exploring the impact of different InfoVis adaptations in the context of digital forensics. However, the focus of this work is to investigate the impact of question complexity and number of nodes, and not the nature of the adaptation.

3.1.1 Participants. We recruited 40 participants with a mean age of 27.2 years ($SD=4.9$) through mailing lists and university portal advertisements. Inclusion criteria required participants to be aged 18 to 65 years, have no history of neurological disorders and have normal or corrected-to-normal vision. Participants also needed to understand and follow the experiment instructions and provide written informed consent before participating.

3.1.2 Stimuli. We consider undirected graphs, to convey information about criminal records, such as numbers of arrests or incarceration states. This is the most common visualization type in this domain [Bohm et al. 2021; Osborne and Slay 2011]. In this environment, nodes represent people, while the edges indicate their relationships. We followed a within-subjects design, where all participants were exposed to all experimental conditions but in randomized order.

We consider two levels of visual complexity: graphs with three (3) or six (6) nodes. Each graph was presented as one of three different configurations:

Baseline: Graphs without any visual adaptation (see example in Figure 1a).

Partial adaptation: Graphs with only one visual adaptation applied (see examples in Figure 1b-Figure 1f).

Full adaptation: Graphs with all adaptations applied simultaneously (see example in Figure 1g).

We consider five possible visual adaptations, based on principles of effective information visualization [Gelman and Unwin 2013; Knoblich et al. 2024; Shen et al. 2021] and popular guidelines,¹ where for example color is used for categorization and size is used to convey quantitative information:

Edge color: Indicates whether individuals share matching birthplaces (Figure 1b).

Edge thickness: Represents the strength of the connection between individuals (Figure 1c).

Node size: Represents the number of arrests made by an individual (Figure 1d).

Node shape: Distinguishes whether the person is currently in jail (Figure 1e).

Node color: Indicates the gender of the individual (Figure 1f).

We prepared a set of questions to assess the participants' ability to interpret the graphs under varying levels of complexity. The questions designed to be answered based on the information conveyed in the graph and were categorized according to their difficulty:

Easy questions: These involved simple queries that required a straightforward interpretation of the graph (e.g., How many people are in jail?).

Hard questions: These required a more in-depth analysis and a higher level of cognitive processing (e.g., How many people with the same birthplace are connected to people with more than two arrests?).

Our independent variables are the numbers of nodes (three and six) and question difficulty (two factors: easy and hard).

3.1.3 Task and Procedure.

Participants completed 15 practice trials to familiarize themselves with the task. The experiment was conducted in a dimly lit room to minimize distractions and optimize eye-tracking data quality. The main experiment consisted of 120 trials per participant (30 for each of our analysed categories). Each trial began with a 1-second fixation cross, followed by a self-paced question-reading phase (Figure 2). Participants then viewed a graph and had 10 seconds to respond before the system advanced to the next trial automatically. Participants provided single-digit responses as quickly and accurately as possible or pressed 'n' if they could not answer. A self-paced resting period followed each trial before proceeding. This cycle repeated for 120 trials, with the experiment lasting about 30 minutes and all trials randomized.

3.1.4 Apparatus. Eye movement data was collected using the GP3 HD Eye Tracker, sampling at 60 Hz in accordance with recommended guidelines [Leiva et al. 2024]. This equipment provides high spatial and temporal resolution, allowing for precise tracking of rapid eye movements [Cuve et al. 2022]. A five-point calibration was conducted for each participant before the study, and it was repeated until minimal error was achieved. Throughout the experiment, various eye movements—including fixations, saccades, and blinks—were recorded. The data collected included timestamps, gaze coordinates (x and y), and eye validity codes, with continuous monitoring of data quality through real-time feedback [Duchowski 2017].

3.2 Generative models

3.2.1 UMSS. Proposed in [Wang et al. 2024a], it involves two main components. The first one produces multi-duration saliency maps for visualization elements and is specifically trained to capture how attention shifts over time based on the visual elements and their

¹<https://datavizcatalogue.com>

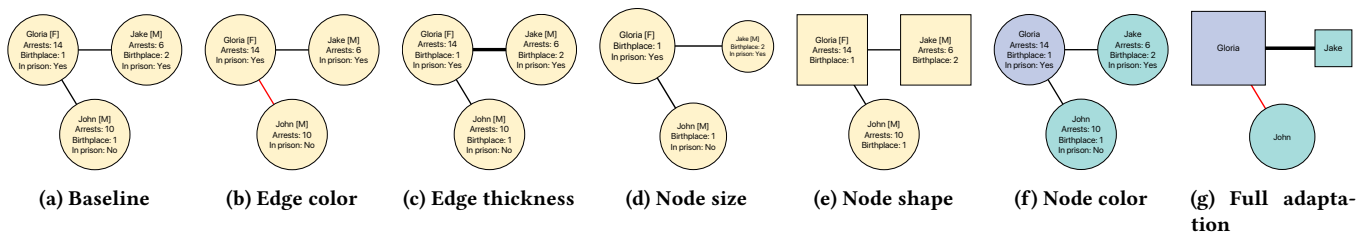


Figure 1: Examples of graph adaptations, from baseline (a) to fully adapted (g) versions. Figures b-f represent the five possible partial adaptations.

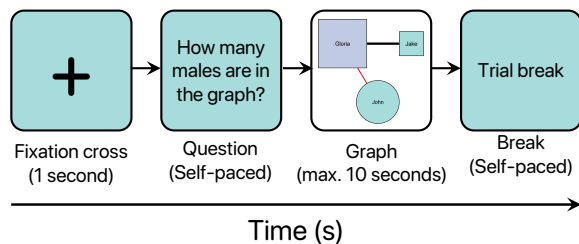


Figure 2: Each trial followed a structured sequence: fixation cross, question screen, graph screen, and resting period. This procedure was repeated for all 120 trials.

relevance at different viewing stages—specifically at 0.5, 3, and 5 seconds. It is based on the model MultiDuration Saliency Excited Model (MD-SEM) [Fosco et al. 2020b] that was proposed for natural images. By calculating the Element Fixation Density (EFD), researchers created the MASSVIS Multi-Duration Element Fixation Density (MASSVIS-MDEFD) using the MASSVIS dataset. This dataset was subsequently utilized to fine-tune MD-SEM, resulting in the development of their Multi-Duration Element Attention Model (MD-EAM). The second component involves Probabilistic Scanpath Sampling using these saliency maps. UMSS probabilistically samples gaze locations to predict the sequence of fixations.

We have successfully replicated their training process and computed both saliency maps and scanpath predictions over a duration of five seconds, consistent with their original implementation. In our images, the stimuli (nodes) are typically positioned at the top or bottom rather than in the center, which makes the initial scanpath sampling algorithm ineffective. To customize the model for our data, we introduce a weighting factor that integrates the saliency prediction with its Gaussian mask during the scanpath sampling process.

3.2.2 DeepGaze++. DeepGaze III [Kümmerer et al. 2022] generates a probabilistic density map for the next fixation based on input images and previously observed fixation points. This approach can produce clusters of closely spaced points, potentially causing stagnation in those regions. To address this issue, DeepGaze++ [Jiang et al. 2023a] iteratively selects the position with the highest probability from the density map and applies a custom inhibition-of-return (IOR) decay to suppress that location in the saliency map. However,

the default IOR decay mechanism is effective only for a limited number of fixations. Therefore, in other research, they adopt the IOR decay introduced in [Emami et al. 2024], which extends coverage beyond 12 fixation points. Furthermore, they integrated the design parameters for this model, which was introduced in the same paper. Despite these adjustments, DeepGaze++ remains a state-of-the-art scanpath model and is thus employed in their investigation. In this paper, we used this model with the IOR method introduced in [Emami et al. 2024], along with the optimal parameters from the same paper.

3.2.3 Gazeformer. Mondal et al. [2023] proposed a transformer-based model for goal-directed human gaze prediction that encodes target objects using a language model, allowing it to generalize to unseen categories (ZeroGaze). The architecture consists of a ResNet-50 [He et al. 2016] backbone for visual feature extraction and RoBERTa [Liu et al. 2019] for target encoding, which are combined into a shared visual-semantic space. A transformer encoder contextualizes the scene, while a transformer decoder predicts fixation sequences in parallel using learnable fixation queries. Fixation locations and durations are directly regressed using a Gaussian distribution-based approach. Training is formulated as a sequence modeling task with a multi-task loss, including L1 regression loss for fixation coordinates and durations, and a negative log-likelihood loss for fixation validity. The model is trained on the COCO-Search18 dataset [Chen et al. 2021].

In our work, we use their available implementation and trained checkpoint. We encode our questions as the task using the language model. Since the model was originally trained to predict up to seven fixations per stimulus, we likewise restrict our analysis to a maximum of seven fixations.

3.3 Metrics

In the case of UMSS and Gazeformer, we generated as many scanpaths per image as there were participants in our study, with the mean evaluation scores representing the averages of all human and predicted scanpath pairs. In contrast, with DeepGaze++, we generated a single scanpath per image. For Gazeformer, we produced seven fixations, as the model is specifically trained to predict this number. In both DeepGaze and UMSS, we generated 12 fixations, reflecting the average fixation count of 12.5 per image in our dataset. We used well-known scanpath prediction metrics used in [Emami et al. 2024].

Question	Graph	DTW (\downarrow)	Eyeanalysis (\downarrow)	Determinism (\uparrow)	Laminarity (\uparrow)
hard	6 nodes	4.3676 ± 0.4010	0.0325 ± 0.0071	1.6162 ± 1.4088	13.3448 ± 5.9174
easy	6 nodes	4.3009 ± 0.5005	0.0352 ± 0.0100	1.0073 ± 0.9065	8.7668 ± 4.0127
hard	3 nodes	4.3414 ± 0.4041	0.0373 ± 0.0077	0.8511 ± 0.7929	8.5293 ± 4.7948
easy	3 nodes	4.1614 ± 0.3345	0.0454 ± 0.0143	0.6084 ± 0.7561	7.0486 ± 4.8389

Table 1: Metrics for the UMSS model (mean & standard deviation) predicting 12 fixations, evaluated by graph complexity and question difficulty.

Question	Graph	DTW (\downarrow)	Eyeanalysis (\downarrow)	Determinism (\uparrow)	Laminarity (\uparrow)
hard	6 nodes	4.7764 ± 0.7233	0.0253 ± 0.0078	5.7138 ± 2.8525	22.3863 ± 7.9269
easy	6 nodes	4.3233 ± 0.8756	0.0315 ± 0.0098	4.7295 ± 2.8249	19.5152 ± 6.1463
hard	3 nodes	4.4060 ± 0.6973	0.0348 ± 0.0085	3.8870 ± 2.2667	13.9008 ± 4.7745
easy	3 nodes	3.6790 ± 0.4919	0.0327 ± 0.0084	3.6320 ± 2.3660	17.8022 ± 4.7747

Table 2: Metrics for the DeepGaze++ model (mean & standard deviation) predicting 12 fixations, evaluated by graph complexity and question difficulty.

Question	Graph	DTW (\downarrow)	Eyeanalysis (\downarrow)	Determinism (\uparrow)	Laminarity (\uparrow)
hard	6 nodes	4.9047 ± 0.9595	0.0392 ± 0.0121	0.3598 ± 0.9258	6.4004 ± 4.3728
easy	6 nodes	3.3858 ± 1.2919	0.0379 ± 0.0161	1.2398 ± 2.2932	7.7372 ± 6.3383
hard	3 nodes	3.5733 ± 1.1852	0.0414 ± 0.0132	0.7707 ± 1.8329	4.3177 ± 3.7336
easy	3 nodes	2.6133 ± 0.7640	0.0421 ± 0.0167	0.9666 ± 2.3136	5.5023 ± 5.1348

Table 3: Metrics for the Gazeformer model (mean & standard deviation) predicting 7 fixations, evaluated by graph complexity and question difficulty.

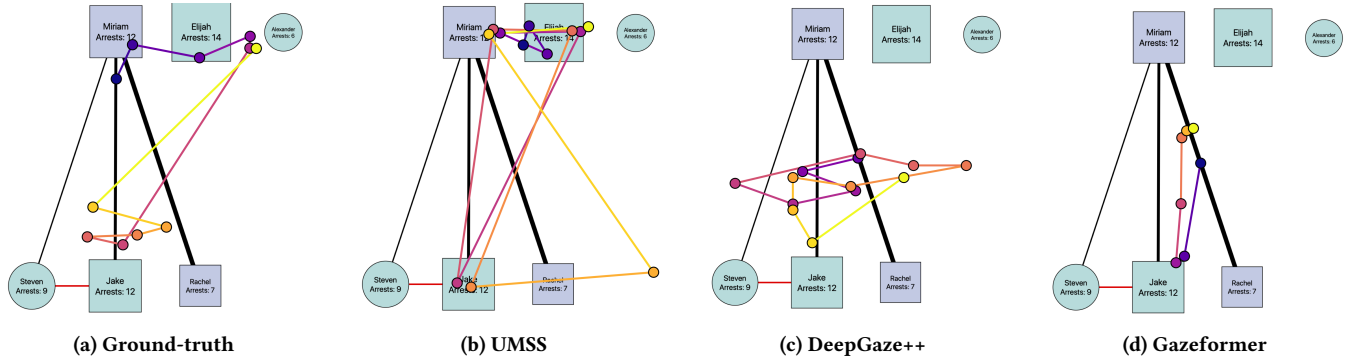


Figure 3: Comparison of scanpaths generated by different models on a graph: (a) Actual eye movement sequence (ground truth); (b–d) Scanpaths predicted by UMSS, DeepGaze++, and Gazeformer, respectively. Colored dots represent fixation points, with connecting lines indicating the fixation order. Color intensity represents the temporal order of fixations, with yellow indicating the first point.

- **Dynamic Time Warping (DTW):** Introduced by Berndt and Clifford [1994], DTW compares time series of varying lengths by calculating a distance matrix and finding the optimal path that adheres to boundary, continuity, and monotonicity constraints. The solution is the minimum-cost path

from the matrix’s start to its endpoint, matching two scanpaths iteratively while including key features [Müller 2007; Wang et al. 2023].

- **Eyeanalysis:** This technique involves double mapping of fixations between two scanpaths to reduce positional variability [Mathôt et al. 2012]. Like DTW, it may assign multiple points from one scanpath to a single point in the other,

identifying the closest fixation points and measuring the average distance between corresponding pairs.

- **Determinism:** This metric evaluates diagonal alignments among cross-recurrent points, representing shared fixation trajectories [Fahimi and Bruce 2021]. With a minimum diagonal length of $l_{\min} = 2$, it measures the percentage of recurrent fixation points in sub-scanpaths, enhancing the original unweighted metric by evaluating congruence in fixation sequences.
- **Laminarity:** Laminarity measures the percentage of fixation points in sub-scanpaths where all corresponding pairs are recurrent, sharing the same fixation point from one scanpath [Anderson et al. 2015; Fahimi and Bruce 2021]. It indicates the tendency of scanpath fixations to cluster in specific locations.

4 Results

The results for the three models, namely UMSS, DeepGaze++, and Gazeformer, are reported in Table 1, Table 2, and Table 3, respectively. The best value for each metric appears in bold, while the second-best is underlined. An example of scanpaths for each model is shown in Figure 3. To ensure a fair comparison, we present the results of UMSS and DeepGaze++ predicting seven fixations in the Appendix A.

DeepGaze++ achieves the highest quantitative performance, though a visual inspection suggests that UMSS generates more plausible scanpaths (Figure 3). UMSS scanpaths contain more fixations on nodes, aligning with findings from Matzen et al. [2018], who observed that models excelling at natural scenes tend to underperform on data visualisations, and vice versa. Specialised InfoVis models tend to focus more on high-information areas [Matzen et al. 2018]. This may explain why Gazeformer exhibits the weakest performance in both quantitative metrics and scanpath plausibility (Figure 3), likely due to its training, which lacks InfoVis data, and its limitation of predicting only seven fixations.

In terms of graph complexity, UMSS and DeepGaze++ perform better with six-node graphs and hard-complexity questions, whereas Gazeformer achieves the best results with six-node graphs and easy questions. In three-node graphs, question complexity has less influence on performance. Notably, Gazeformer, the only model that explicitly encodes the question, achieves relatively strong results despite its disadvantages, suggesting that question incorporation plays a role in scanpath prediction.

The evaluated metrics are sensitive to both the number of nodes in the graph and question complexity. Performance improves with six-node stimuli, even when all models predict only seven fixations (Appendix A). This likely occurs because three-node graphs contain less information than the datasets used to train these models.

Moreover, we find that scanpath predictions are significantly influenced by the training datasets of each model, as well as model-specific parameters such as the number of fixations and internal configuration settings. As Emami et al. [2024] highlight, certain parameters heavily impact predictions and are not easily optimised. For example, as shown in Appendix A.1 and Appendix A.2, both UMSS and DeepGaze++ exhibit metric variations, particularly in DTW, depending on the number of predicted fixations. Additionally,

to generate plausible scanpaths with UMSS, we had to adapt the algorithm to our specific visualization type (subsubsection 3.2.1).

After analysing these three state-of-the-art models—two selected based on their training datasets and one for its ability to incorporate questions—we concluded that using a pretrained scanpath generation model requires careful parameter optimization and potentially fine-tuning to be effective on a new dataset.

5 Limitations and future work

When evaluating the models, we did not perform fine-tuning or an exhaustive search for the best parameters. We replicated training or used pretrained checkpoints when available, although with some modifications to adapt them to our data, especially in the case of UMSS.

As future work, it would be interesting to explore how the performance of these models improves when fine-tuned with this dataset. In particular, Gazeformer could be further optimized by training it to predict more than seven fixations and by adapting it specifically for this task. For instance, the model could benefit from fine-tuning the ResNet module used for feature extraction, as it is not optimized for InfoVis images, which differ significantly from the images it was originally trained on. Also, investigate models such as Chartist [Shi et al. 2025] to assess their generalization capabilities on our task and visualization type, different from their training data.

As a complementary analysis, it would be interesting to examine whether user response accuracy affects model performance. Specifically, we could study whether the models predict scanpaths more effectively in trials where the question was answered correctly versus incorrectly.

Ethical statement

We obtained informed consent from the participants, ensuring the anonymization of their data. Consequently, the ET datasets collected in this study provide anonymous records in compliance with ethical board approvals, containing no personal information. This approach guarantees the privacy and anonymity of the collected data. To address potential privacy concerns associated with ET data collection and processing, the datasets presented are unlinkable to individual participants, thus preventing any possible misuse.

Acknowledgments

This research is supported by Horizon Europe’s European Innovation Council through the Pathfinder program (SYMBIOTIK project, grant 101071147) and by the Industrial Doctorate Plan of the Department of Research and Universities of the Generalitat de Catalunya, under Grant AGAUR 2023 DI060.

References

- Nicola C Anderson, Fraser Anderson, Alan Kingstone, and Walter F Bischof. 2015. A comparison of scanpath comparison methods. *Behavior research methods* 47 (2015), 1377–1392.
- Marc Assens, Xavier Giro-i Nieto, Kevin McGuinness, and Noel E. O’Connor. 2018. PathGAN: Visual Scanpath Prediction with Generative Adversarial Networks. doi:10.48550/arXiv.1809.00567 arXiv:1809.00567.
- Marc Assens, Xavier Giro-i Nieto, Kevin McGuinness, and Noel E. O’Connor. 2017. SaltiNet: Scan-Path Prediction on 360 Degree Images Using Saliency Volumes. In *2017 IEEE International Conference on Computer Vision Workshops (ICCVW)*. 2331–2338. doi:10.1109/ICCVW.2017.275 ISSN: 2473-9944.

- Bahar Aydemir, Ludo Hoffstetter, Tong Zhang, Mathieu Salzmann, and Sabine Süsstrunk. 2023. TempSAL - Uncovering Temporal Information for Deep Saliency Prediction. In *2023 IEEE/CVF Conference on Computer Vision and Pattern Recognition (CVPR)*. IEEE, Vancouver, BC, Canada, 6461–6470. doi:10.1109/CVPR52729.2023.00625
- Donald J Berndt and James Clifford. 1994. Using dynamic time warping to find patterns in time series. In *Proceedings of the 3rd international conference on knowledge discovery and data mining*. 359–370.
- Fabian Bohm, Ludwig Englbrecht, Sabrina Friedl, and Gunther Pernul. 2021. Visual Decision-Support for Live Digital Forensics. In *Proc. VizSec*.
- Ali Borji and Laurent Itti. 2015. CAT2000: A Large Scale Fixation Dataset for Boosting Saliency Research. doi:10.48550/arXiv.1505.03581 arXiv:1505.03581 [cs].
- Michelle A. Borkin, Zoya Bylinskii, Nam Wook Kim, Constance May Bainbridge, Chelsea S. Yeh, Daniel Borkin, Hanspeter Pfister, and Aude Oliva. 2016. Beyond Memorability: Visualization Recognition and Recall. *IEEE Transactions on Visualization and Computer Graphics* 22, 1 (Jan. 2016), 519–528. doi:10.1109/TVCG.2015.2467732 IEEE Transactions on Visualization and Computer Graphics.
- Giuseppe Cartella, Marcella Cornia, Vittorio Cuculo, Alessandro D’Amelio, Dario Zanca, Giuseppe Boccignone, and Rita Cucchiara. 2024. Trends, Applications, and Challenges in Human Attention Modelling. Vol. 9. 7971–7979. doi:10.24963/ijcai.2024/882 ISSN: 1045-0823.
- Shi Chen, Nachiappan Valliappan, Shaolei Shen, Xinyu Ye, Kai Kohlhoff, and Junfeng He. 2023. Learning from Unique Perspectives: User-aware Saliency Modeling. In *2023 IEEE/CVF Conference on Computer Vision and Pattern Recognition (CVPR)*. IEEE, Vancouver, BC, Canada, 2701–2710. doi:10.1109/CVPR52729.2023.00265
- Yupei Chen, Zhibo Yang, Seoyoung Ahn, Dimitris Samaras, Minh Hoai, and Gregory Zelinsky. 2021. COCO-Search18 fixation dataset for predicting goal-directed attention control. *Scientific Reports* 11, 1 (April 2021), 8776. doi:10.1038/s41598-021-87715-9 Publisher: Nature Publishing Group.
- Hélio Clemente Cuve, Jelka Stojanov, Xavier Roberts-Gaal, Caroline Catmur, and Geoffrey Bird. 2022. Validation of Gazepoint low-cost eye-tracking and psychophysical bundle. *Behavior research methods* 54, 2 (2022), 1027–1049.
- Alessandro D’Amelio, Giuseppe Cartella, Vittorio Cuculo, Manuele Lucchi, Marcella Cornia, Rita Cucchiara, and Giuseppe Boccignone. 2024. TPP-Gaze: Modelling Gaze Dynamics in Space and Time with Neural Temporal Point Processes. doi:10.48550/arXiv.2410.23409 arXiv:2410.23409.
- Shuwen Deng, David R. Reich, Paul Prasse, Patrick Haller, Tobias Scheffer, and Lena A. Jäger. 2023. Eyettention: An Attention-based Dual-Sequence Model for Predicting Human Scanpaths during Reading. *Proc. ACM Hum.-Comput. Interact.* 7, ETRA (May 2023). doi:10.1145/3591131 Place: New York, NY, USA Publisher: Association for Computing Machinery.
- Andrew T Duchowski. 2017. *Eye tracking methodology: Theory and practice*. Springer.
- Parvin Emami, Yue Jiang, Zixin Guo, and Luis A. Leiva. 2024. Impact of Design Decisions in Scanpath Modeling. *Proc. ACM Hum.-Comput. Interact.* 8, ETRA (May 2024), 1–16. doi:10.1145/3655602
- Ramin Fahimi and Neil DB Bruce. 2021. On metrics for measuring scanpath similarity. *Behavior Research Methods* 53 (2021), 609–628.
- Stephen H. Fairclough. 2022. *Current research in neuroadaptive technology*. Academic Press, Chapter Designing human-computer interaction with neuroadaptive technology.
- Camilo Fosco, Vincent Casser, Amish Kumar Bedi, Peter O’Donovan, Aaron Hertzmann, and Zoya Bylinskii. 2020a. Predicting Visual Importance Across Graphic Design Types. In *Proceedings of the 33rd Annual ACM Symposium on User Interface Software and Technology*. ACM, Virtual Event USA, 249–260. doi:10.1145/3379337.3415825
- Camilo Fosco, Analise Newman, Pat Sukhum, Yun Bin Zhang, Nanxuan Zhao, Aude Oliva, and Zoya Bylinskii. 2020b. How Much Time Do You Have? Modeling Multi-Duration Saliency. In *2020 IEEE/CVF Conference on Computer Vision and Pattern Recognition (CVPR)*. IEEE, Seattle, WA, USA, 4472–4481. doi:10.1109/CVPR42600.2020.00453
- Andrew Gelman and Antony Unwin. 2013. Infovis and Statistical Graphics: Different Goals, Different Looks. *J. Comput. Graph. Stat.* 22 (2013).
- Syrine Haddad, Kayhan Latifzadeh, Saravanakumar Duraisamy, Jean Vanderdonckt, Olfa Daassi, Safya Belghith, and Luis A. Leiva. 2024. Good GUIs, Bad GUIs: Affective Evaluation of Graphical User Interfaces. In *Proc. UMAP*.
- Kaiming He, Xiangyu Zhang, Shaoqing Ren, and Jian Sun. 2016. Deep Residual Learning for Image Recognition. In *2016 IEEE Conference on Computer Vision and Pattern Recognition (CVPR)*. 770–778. doi:10.1109/CVPR.2016.90
- Leanne M Hirshfield, Rebecca Golotta, Stuart Hirshfield, Sam Hincks, Matthew Russell, Rachel Ward, Tom Williams, and Robert Jacob. 2011. This is your brain on interfaces: enhancing usability testing with functional near-infrared spectroscopy. In *Proc. CHI*.
- Ming Jiang, Shengsheng Huang, Juanyong Duan, and Qi Zhao. 2015. SALICON: Saliency in Context. In *2015 IEEE Conference on Computer Vision and Pattern Recognition (CVPR)*. 1072–1080. doi:10.1109/CVPR.2015.7298710 ISSN: 1063-6919.
- Yue Jiang, Luis A. Leiva, Hamed Rezazadegan Tavakoli, Paul R. B. Houssel, Julia Kymälä, and Antti Oulasvirta. 2023a. UEye: Understanding Visual Saliency across User Interface Types. In *Proceedings of the 2023 CHI Conference on Human Factors in Computing Systems (CHI ’23)*. Association for Computing Machinery, New York, NY, USA, 1–21. doi:10.1145/3544548.3581096
- Yue Jiang, Luis A. Leiva, Hamed Rezazadegan Tavakoli, Paul RB Houssel, Julia Kymälä, and Antti Oulasvirta. 2023b. UEye: Understanding Visual Saliency across User Interface Types. In *Proceedings of the 2023 CHI Conference on Human Factors in Computing Systems*. 1–21.
- Varun Khurana, Yaman Kumar, Nora Hollenstein, Rajesh Kumar, and Balaji Krishnamurthy. 2023. Synthesizing Human Gaze Feedback for Improved NLP Performance. Andreas Vlachos and Isabelle Augenstein (Eds.). Association for Computational Linguistics, Dubrovnik, Croatia, 1895–1908. doi:10.18653/v1/2023.eacl-main.139
- Nam Wook Kim, Zoya Bylinskii, Michelle A. Borkin, Krzysztof Z. Gajos, Aude Oliva, Fredo Durand, and Hanspeter Pfister. 2017. BubbleView: An Interface for Crowdsourcing Image Importance Maps and Tracking Visual Attention. *ACM Trans. Comput.-Hum. Interact.* 24, 5 (Nov. 2017), 36:1–36:40. doi:10.1145/3131275
- Steven Knoblich, Jan Mendling, and Helena Jambor. 2024. Review of visual encodings in common process mining tools. In *Proc. VIPRA Workshop*.
- Matthias Kümmerer, Matthias Bethge, and Thomas S. A. Wallis. 2022. DeepGaze III: Modeling free-viewing human scanpaths with deep learning. *Journal of Vision* 22, 5 (April 2022), 7. doi:10.1167/jov.22.5.7
- Luis A. Leiva, Javier Traver, Alexandra Kawala-Sterniuk, and Tuukka Ruotsalo. 2024. Modeling User Preferences via Brain-Computer Interfacing. *arXiv preprint arXiv:2405.09691* (2024).
- Peizhao Li, Junfeng He, Gang Li, Rachit Bhargava, Shaolei Shen, Nachiappan Valliappan, Youwei Liang, Hongxiang Gu, Venky Ramachandran, Golnaz Farhadi, Yang Li, Kai J. Kohlhoff, and Vidhya Navalpakkam. 2024. UniAR: A Unified model for predicting human Attention and Responses on visual content. <https://openreview.net/forum?id=FjssnGuHih¬id=n31VtGnAO9>
- Yinhan Liu, Myle Ott, Naman Goyal, Jingfei Du, Mandar Joshi, Danqi Chen, Omer Levy, Mike Lewis, Luke Zettlemoyer, and Veselin Stoyanov. 2019. RoBERTa: A Robustly Optimized BERT Pretraining Approach. doi:10.48550/arXiv.1907.11692 arXiv:1907.11692 [cs].
- Kristiyan Lukanov, Horia A. Maior, and Max L. Wilson. 2016. Using fNIRS in Usability Testing: Understanding the Effect of Web Form Layout on Mental Workload. In *Proc. CHI*.
- Daniel Martin, Ana Serrano, Alexander W. Bergman, Gordon Wetzstein, and Belen Masia. 2022. ScanGAN360: A Generative Model of Realistic Scanpaths for 360° Images. *IEEE Transactions on Visualization and Computer Graphics* 28, 5 (May 2022), 2003–2013. doi:10.1109/TVCG.2022.3150502 Conference Name: IEEE Transactions on Visualization and Computer Graphics.
- Sebastian Mathôt, Filipe Cristino, Iain D Gilchrist, and Jan Theeuwes. 2012. A simple way to estimate similarity between pairs of eye movement sequences. *Journal of Eye Movement Research* 5, 1 (2012), 1–15.
- Laura E. Matzen, Michael J. Haass, Kristin M. Divis, Zhiyuan Wang, and Andrew T. Wilson. 2018. Data Visualization Saliency Model: A Tool for Evaluating Abstract Data Visualizations. *IEEE Transactions on Visualization and Computer Graphics* 24, 1 (Jan. 2018), 563–573. doi:10.1109/TVCG.2017.2743939
- Sounak Mondal, Zhibo Yang, Seoyoung Ahn, Dimitris Samaras, Gregory Zelinsky, and Minh Hoai. 2023. Gazeformer: Scalable, Effective and Fast Prediction of Goal-Directed Human Attention. In *2023 IEEE/CVF Conference on Computer Vision and Pattern Recognition (CVPR)*. IEEE, Vancouver, BC, Canada, 1441–1450. doi:10.1109/CVPR52729.2023.00145
- Meinard Müller. 2007. Dynamic time warping. *Information retrieval for music and motion* (2007), 69–84.
- Truong-Huy D. Nguyen, Magy Seif El-Nasr, and Derek M. Isaacowitz. 2017. Interactive Visualization for Understanding of Attention Patterns. In *Eye Tracking and Visualization*, Michael Burch, Lewis Chuang, Brian Fisher, Albrecht Schmidt, and Daniel Weiskopf (Eds.). Springer International Publishing, Cham, 23–39.
- Grant Osborne and Jill Slay. 2011. Digital Forensics Infovis: An implementation of a process for visualisation of digital evidence. In *Proc. ARES*.
- Evan M M. Peck, Beste F. Yuksel, Alvitta Ottley, Robert J.K. Jacob, and Remco Chang. 2013. Using fNIRS brain sensing to evaluate information visualization interfaces. In *Proc. CHI*.
- Lisa Perkhofer, Othmar M. Lehner, and Horst Treiblmaier. 2016. InfoVis: The Impact of Information Overload on Decision Making Outcome in High Complexity Settings. In *Proc. CHI*.
- Patrik Polatsek, Manuela Waldner, Ivan Viola, Peter Kapeck, and Wanda Benesova. 2018. Exploring visual attention and saliency modeling for task-based visual analysis. *Computers & Graphics* 72 (May 2018), 26–38. doi:10.1016/j.cag.2018.01.010
- Leixian Shen, Enya Shen, Zhiwei Tai, Yiran Song, and Jianmin Wang. 2021. TaskVis: Task-oriented Visualization Recommendation. In *Proc. EuroVis*.
- Danqing Shi, Yao Wang, Yunpeng Bai, Andreas Bulling, and Antti Oulasvirta. 2025. Chartist: Task-driven Eye Movement Control for Chart Reading. doi:10.48550/arXiv.2502.03575 arXiv:2502.03575 [cs].
- Xiangjie Sui, Yuming Fang, Hanwei Zhu, Shiqi Wang, and Zhou Wang. 2023. ScanDMM: A Deep Markov Model of Scanpath Prediction for 360° Images. In *2023 IEEE/CVF Conference on Computer Vision and Pattern Recognition (CVPR)*. IEEE, Vancouver, BC, Canada, 6989–6999. doi:10.1109/CVPR52729.2023.00675
- Xiaowei Wang, Xubo Li, Haiying Wang, Wenning Zhao, and Xia Liu. 2023. An Improved Dynamic Time Warping Method Combining Distance Density Clustering for Eye

- Movement Analysis. *Journal of Mechanics in Medicine and Biology* 23, 02 (2023), 2350031.
- Yao Wang, Mihai Băce, and Andreas Bulling. 2024a. Scanpath Prediction on Information Visualisations. *IEEE Trans. Visual. Comput. Graphics* 30, 7 (July 2024), 3902–3914. doi:10.1109/TVCG.2023.3242293
- Yao Wang, Weitian Wang, Abdullah Abdelhafez, Mayar Elfars, Zhiming Hu, Mihai Băce, and Andreas Bulling. 2024b. SalChartQA: Question-driven Saliency on Information Visualisations. In *Proceedings of the 2024 CHI Conference on Human Factors in Computing Systems (CHI '24)*. Association for Computing Machinery, New York, NY, USA, 1–14. doi:10.1145/3613904.3642942

Appendix

A Additional results

A.1 UMSS

In Table 4, we present the results of UMSS predicting seven fixations. Additionally, we filter the organic data to include only the first seven fixations and we recompute metrics in Table 5. We do the same process for 12 fixations in Table 6 and Table 7. The difference in metrics according to the question and the number of nodes is consistent, predicting a different number of fixations. DTW is the metric most affected by both the number of fixations and filtering organic data to the same number of fixations as in the predicted sequence of scanpaths. DTW achieves better values when the number of fixations is similar between the two compared sequences.

A.2 DeepGaze++

In Table 8, we present the results of DeepGaze++ predicting seven fixations. Additionally, we filter the organic data to include only the first seven fixations and we recompute metrics in Table 9. We do the same process for 12 fixations in Table 10 and Table 11. Similarly as explained in subsection A.1, the most affected metric by filtering is DTW.

A.3 Gazeformer

In Table 12, we present the results of Gazeformer predicting seven fixations. Additionally, we filter the organic data to include only the first seven fixations and we recompute metrics in Table 13.

Question	Graph	DTW (\downarrow)	Eyeanalysis (\downarrow)	Determinism (\uparrow)	Laminarity (\uparrow)
hard	6 nodes	3.7558 ± 0.3765	0.0387 ± 0.0097	0.5465 ± 0.6692	7.3626 ± 3.7459
easy	6 nodes	3.4907 ± 0.5743	0.0432 ± 0.0116	0.3046 ± 0.3219	5.1789 ± 3.2532
hard	3 nodes	3.5266 ± 0.4808	0.0475 ± 0.0117	0.1962 ± 0.2947	4.7403 ± 3.2299
easy	3 nodes	3.0397 ± 0.4084	0.0542 ± 0.0131	0.2104 ± 0.2948	4.8477 ± 3.8996

Table 4: Metrics for the UMSS model (mean & standard deviation) predicting 7 fixations, evaluated by graph complexity and question difficulty.

Question	Graph	DTW (\downarrow)	Eyeanalysis (\downarrow)	Determinism (\uparrow)	Laminarity (\uparrow)
hard	6 nodes	2.3068 ± 0.2620	0.0483 ± 0.0100	0.5465 ± 0.6692	7.3626 ± 3.7459
easy	6 nodes	2.4121 ± 0.3016	0.0548 ± 0.0140	0.3046 ± 0.3219	5.1789 ± 3.2532
hard	3 nodes	2.6027 ± 0.1689	0.0586 ± 0.0068	0.1962 ± 0.2947	4.7403 ± 3.2299
easy	3 nodes	2.5613 ± 0.1503	0.0620 ± 0.0096	0.2104 ± 0.2948	4.8477 ± 3.8996

Table 5: Metrics for the UMSS model (mean & standard deviation) predicting 7 fixations, evaluated by graph complexity and question difficulty, filtering organic data based on the first 7 fixations.

Question	Graph	DTW (\downarrow)	Eyeanalysis (\downarrow)	Determinism (\uparrow)	Laminarity (\uparrow)
hard	6 nodes	4.3676 ± 0.4010	0.0325 ± 0.0071	1.6162 ± 1.4088	13.3448 ± 5.9174
easy	6 nodes	4.3009 ± 0.5005	0.0352 ± 0.0100	1.0073 ± 0.9065	8.7668 ± 4.0127
hard	3 nodes	4.3414 ± 0.4041	0.0373 ± 0.0077	0.8511 ± 0.7929	8.5293 ± 4.7948
easy	3 nodes	4.1614 ± 0.3345	0.0454 ± 0.0143	0.6084 ± 0.7561	7.0486 ± 4.8389

Table 6: Metrics for the UMSS model (mean & standard deviation) predicting 12 fixations, evaluated by graph complexity and question difficulty.

Question	Graph	DTW (\downarrow)	Eyeanalysis (\downarrow)	Determinism (\uparrow)	Laminarity (\uparrow)
hard	6 nodes	3.8517 ± 0.3717	0.0366 ± 0.0074	1.6162 ± 1.4088	13.3448 ± 5.9174
easy	6 nodes	3.9480 ± 0.4351	0.0391 ± 0.0095	1.0073 ± 0.9065	8.7668 ± 4.0127
hard	3 nodes	4.0980 ± 0.3104	0.0399 ± 0.0067	0.8511 ± 0.7929	8.5293 ± 4.7948
easy	3 nodes	4.0598 ± 0.3011	0.0467 ± 0.0139	0.6084 ± 0.7561	7.0486 ± 4.8389

Table 7: Metrics for the UMSS model (mean & standard deviation) predicting 12 fixations, evaluated by graph complexity and question difficulty, filtering organic data based on the first 12 fixations.

Question	Graph	DTW (\downarrow)	Eyeanalysis (\downarrow)	Determinism (\uparrow)	Laminarity (\uparrow)
hard	6 nodes	4.4279 ± 0.7542	0.0296 ± 0.0086	5.2506 ± 2.7208	21.6753 ± 7.7796
easy	6 nodes	3.6398 ± 0.9210	0.0355 ± 0.0101	4.5245 ± 3.0246	19.7765 ± 6.2049
hard	3 nodes	3.7249 ± 0.8538	0.0392 ± 0.0112	3.2529 ± 2.6520	14.1096 ± 4.8151
easy	3 nodes	2.8477 ± 0.5451	0.0350 ± 0.0100	3.4354 ± 2.1081	17.8470 ± 4.9186

Table 8: Metrics for the DeepGaze++ model (mean & standard deviation) predicting 7 fixations, evaluated by graph complexity and question difficulty.

Question	Graph	DTW (\downarrow)	Eyeanalysis (\downarrow)	Determinism (\uparrow)	Laminarity (\uparrow)
hard	6 nodes	2.1105 \pm 0.2562	0.0264 \pm 0.0077	4.8746 \pm 3.5018	20.4399 \pm 6.7628
easy	6 nodes	2.3628 \pm 0.3176	0.0350 \pm 0.0096	4.4420 \pm 3.0489	19.2532 \pm 6.1302
hard	3 nodes	2.4614 \pm 0.3535	0.0369 \pm 0.0110	3.2124 \pm 2.5604	14.1334 \pm 5.3275
easy	3 nodes	2.2919 \pm 0.3018	0.0335 \pm 0.0098	3.6108 \pm 2.2370	18.1738 \pm 5.3647

Table 9: Metrics for the DeepGaze++ model (mean & standard deviation) predicting 7 fixations, evaluated by graph complexity and question difficulty, filtering organic data based on the first 7 fixations.

Question	Graph	DTW (\downarrow)	Eyeanalysis (\downarrow)	Determinism (\uparrow)	Laminarity (\uparrow)
hard	6 nodes	4.7764 \pm 0.7233	0.0253 \pm 0.0078	5.7138 \pm 2.8525	22.3863 \pm 7.9269
easy	6 nodes	4.3233 \pm 0.8756	0.0315 \pm 0.0098	4.7295 \pm 2.8249	19.5152 \pm 6.1463
hard	3 nodes	4.4060 \pm 0.6973	0.0348 \pm 0.0085	3.8870 \pm 2.2667	13.9008 \pm 4.7745
easy	3 nodes	3.6790 \pm 0.4919	0.0327 \pm 0.0084	3.6320 \pm 2.3660	17.8022 \pm 4.7747

Table 10: Metrics for the DeepGaze++ model (mean & standard deviation) predicting 12 fixations, evaluated by graph complexity and question difficulty.

Question	Graph	DTW (\downarrow)	Eyeanalysis (\downarrow)	Determinism (\uparrow)	Laminarity (\uparrow)
hard	6 nodes	3.3961 \pm 0.4109	0.0250 \pm 0.0069	5.4042 \pm 2.9753	21.8460 \pm 7.6795
easy	6 nodes	3.6931 \pm 0.5609	0.0321 \pm 0.0099	4.5699 \pm 2.9623	19.6052 \pm 6.3182
hard	3 nodes	3.8254 \pm 0.4870	0.0342 \pm 0.0090	3.3734 \pm 2.2944	13.9846 \pm 4.8498
easy	3 nodes	3.4742 \pm 0.4003	0.0324 \pm 0.0084	3.3515 \pm 2.0423	17.7992 \pm 4.9506

Table 11: Metrics for the DeepGaze++ model (mean & standard deviation) predicting 12 fixations, evaluated by graph complexity and question difficulty, filtering organic data based on the first 12 fixations.

Question	Graph	DTW (\downarrow)	Eyeanalysis (\downarrow)	Determinism (\uparrow)	Laminarity (\uparrow)
hard	6 nodes	4.9047 \pm 0.9595	0.0392 \pm 0.0121	0.3598 \pm 0.9258	6.4004 \pm 4.3728
easy	6 nodes	3.3858 \pm 1.2919	0.0379 \pm 0.0161	1.2398 \pm 2.2932	7.7372 \pm 6.3383
hard	3 nodes	3.5733 \pm 1.1852	0.0414 \pm 0.0132	0.7707 \pm 1.8329	4.3177 \pm 3.7336
easy	3 nodes	2.6133 \pm 0.7640	0.0421 \pm 0.0167	0.9666 \pm 2.3136	5.5023 \pm 5.1348

Table 12: Metrics for the Gazeformer model (mean & standard deviation) predicting 7 fixations, evaluated by graph complexity and question difficulty.

Question	Graph	DTW (\downarrow)	Eyeanalysis (\downarrow)	Determinism (\uparrow)	Laminarity (\uparrow)
hard	6 nodes	2.4586 \pm 0.5782	0.0555 \pm 0.0223	0.3598 \pm 0.9258	6.4004 \pm 4.3728
easy	6 nodes	2.1863 \pm 0.7229	0.0490 \pm 0.0246	1.2398 \pm 2.2932	7.7372 \pm 6.3383
hard	3 nodes	2.3663 \pm 0.5949	0.0519 \pm 0.0213	0.7707 \pm 1.8329	4.3177 \pm 3.7336
easy	3 nodes	2.1944 \pm 0.5489	0.0504 \pm 0.0221	0.9666 \pm 2.3136	5.5023 \pm 5.1348

Table 13: Metrics for the Gazeformer model (mean & standard deviation) predicting 7 fixations, evaluated by graph complexity and question difficulty, filtering organic data based on the first 7 fixations.